The EMBO Journal (2006) 25, 2420–2431 | © 2006 European Molecular Biology Organization | All Rights Reserved 0261-4189/06
www.embojournal.org

THE
EMBO
JOURNAL

Histone H2B mutations in inner region affect ubiquitination, centromere function, silencing and chromosome segregation

Takeshi Maruyama, Takahiro Nakamura, Takeshi Hayashi and Mitsuhiro Yanagida*

Department of Gene Mechanisms, Graduate School of Biostudies, Kyoto University, Yoshida-Honmachi, Sakyo-ku, Kyoto, Japan

The reiterated nature of histone genes has hampered genetic approach to dissect the role of histones in chromatin dynamics. We here report isolation of three temperature-sensitive (*ts*) *Schizosaccharomyces pombe* strains, containing amino-acid substitutions in the sole histone H2B gene (*htb1*$^+$). The mutation sites reside in the highly conserved, non-helical residues of H2B, which are implicated in DNA–protein or protein–protein interactions in the nucleosome. In the allele of *htb1-72*, the substitution (G52D) occurs at the DNA binding loop L1, causing disruption of the gene silencing in heterochromatic regions and lagging chromosomes in anaphase. In another allele *htb1-223* (P102L) locating in the junction between α3 and αC, the mutant residue is in contact with H2A and other histones, leading to structural aberrations in the central centromere chromatin and unequal chromosome segregation in anaphase. The third allele *htb1-442* (E34K) near α1 displayed little defect. Evidence is provided that monoubiquitinated H2B is greatly unstable in P102L mutant, possibly owing to proteasome-independent destruction or enhanced deubiquitination. Histone H2B thus plays an important role in centromere/kinetochore formation.

The EMBO Journal (2006) **25,** 2420–2431. doi:10.1038/sj.emboj.7601110; Published online 11 May 2006
Subject Categories: chromatin & transcription
Keywords: centromere; chromatin; gene silencing; histone H2B; monoubiquitination

Introduction

In eukaryotic cells, DNA is packaged repetitively into nucleosomes by means of interactions among four classes of histones, H2A, H2B, H3 and H4 (Richmond *et al*, 1984; van Holde, 1988; Kornberg and Lorch, 1999; Elgin and Workman, 2002). The crystal structure of the nucleosome core particle consists of approximately 147 bp of DNA organized into a superhelix around an octamer of two of each of these four histones (Luger *et al*, 1997; Luger, 2003; Richmond and Davey, 2003). Histones are phosphorylated, acetylated, methylated, ubiquitinated and sumoylated (Peterson and Laniel, 2004). Extensive post-translational modifications mainly occur in the tail regions of histones, and affect transcriptional activation, repression, chromatin assembly, heterochromatin gene silencing, centromere chromatin, response to DNA damages, histone deposition, chromosome segregation, mitosis, meiosis and spermatogenesis: histone tails may be viewed as complex protein–protein interaction surface that are regulated by numerous modifications (e.g., Grewal and Elgin, 2002; Fischle *et al*, 2003a, b; Hayashi *et al*, 2004; Korber and Horz, 2004; Tagami *et al*, 2004).

Histone tails contribute significantly neither to the structure of individual nucleosomes nor to the stability, but they are thought to strongly affect the folding of nucleosomal arrays into higher-order structure. What then would be the role of inner histone structure in cellular physiological regulations? Does it solely contribute toward the assembly to nucleosomal structure? Post-translational modifications infrequently occur in the inner structure, which is often not exposed to the outer surface of nucleosome. However, K79 in the L1 region between α1 and α2 of H3 (L and α represent, respectively, loop and α-helix; Luger *et al*, 1997) is methylated by a methylase Dot1 and this methylation has been shown to be implicated in meiotic checkpoint control and telomeric silencing (San-Segundo and Roeder, 2000; Feng *et al*, 2002; Ng *et al*, 2002; van Leeuwen *et al*, 2002). Amino-acid substitution mutants in the inner histone structure have been scarce, as genetic analyses of histone functions in metazoan cells are hampered because of the high copy numbers of the histone genes in the genome.

In this study, we characterized the temperature-sensitive (*ts*) mutants of the fission yeast *Schizosaccharomyces pombe* histone H2B gene. The mutation sites reside in the highly conserved, non-helical, inner regions of histone H2B. Our results suggested that the inner structure of H2B is essential for proper ubiquitination, centromere function, gene silencing and chromosome segregation.

Results

Isolation of S. pombe histone H2B mutants

To isolate histone H2B mutants, *ts* mutants were randomly isolated, followed by characterization of cytological mutant phenotypes (Hayashi *et al*, 2004). Then, mass transformation using plasmid pH2AH2B that carried the paired genes of histone H2A–H2B (Yuasa *et al*, 2004) was performed by introducing plasmid into ~500 individual strains. The resulting transformants were screened for their ability to produce colonies at the restrictive temperature (36°C). Three mutant strains (72, 223, 442), whose *ts* phenotype was fully suppressed by plasmid pH2AH2B at 36°C, were obtained. Subcloning established that the histone H2B gene (designated *htb1*$^+$: Matsumoto and Yanagida, 1985), but not H2A gene, was capable of suppressing the *ts* phenotype (Figure 1A).

*Corresponding author. Department of Gene Mechanisms, Graduate School of Biostudies, Kyoto University, Yoshida-Honmachi, Sakyo-ku, Kyoto 606-8501, Japan. Tel.: +81 75 753 4205; Fax: +81 75 753 4208; E-mail: yanagida@kozo.biophys.kyoto-u.ac.jp

Received: 22 August 2005; accepted: 3 April 2006; published online: 11 May 2006

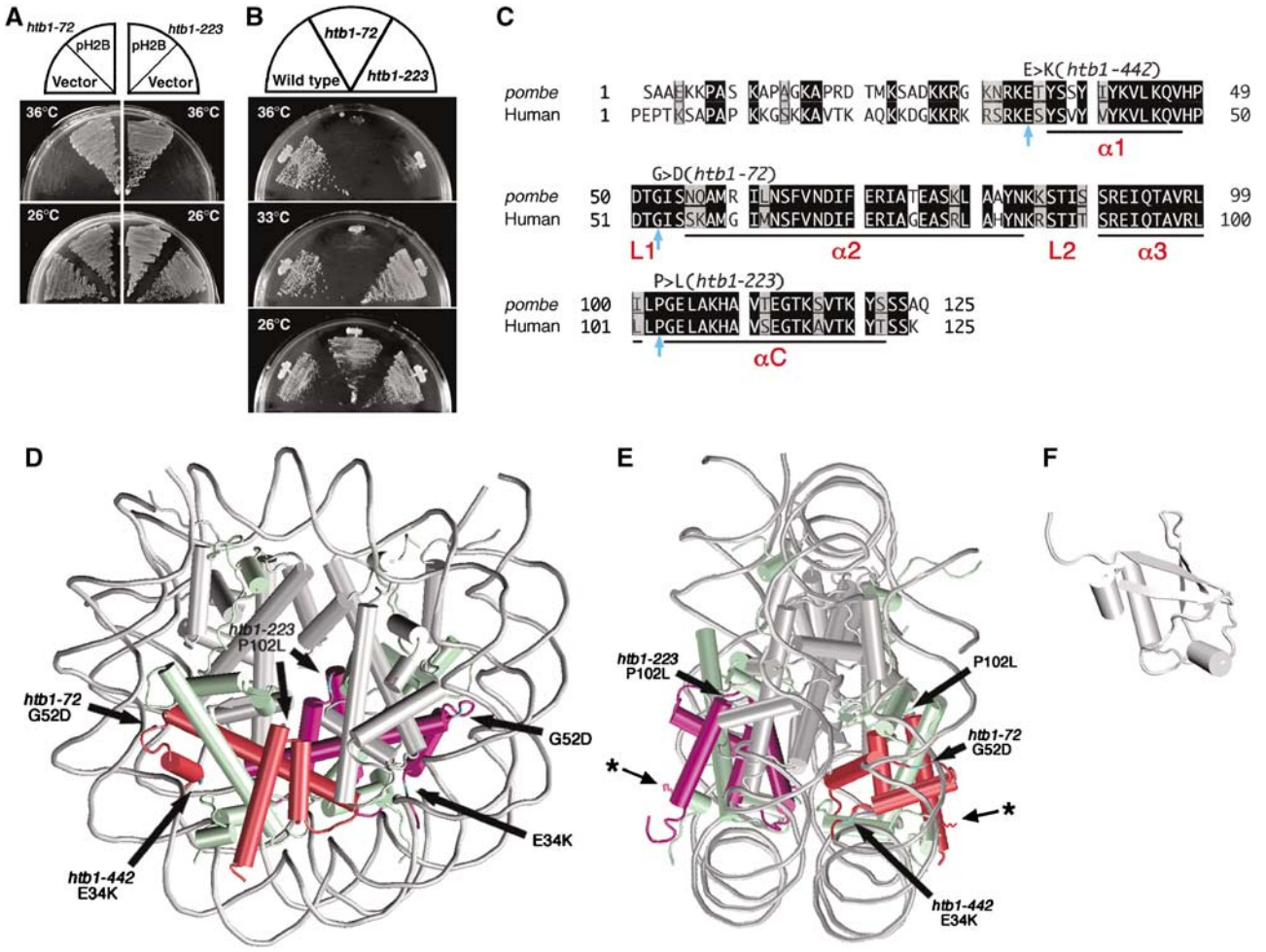

Figure 1 *S. pombe* H2B mutations reside in the conserved, non-helical regions. (**A**) Plasmid pH2B suppresses the *ts* phenotype of *htb1-72* and *htb1-223*. (**B**) *htb1-72* and *htb1-223* mutants fail to produce colonies at 36°C on the complete YPD plates. (**C**) Amino-acid sequences of fission yeast and human histone H2B. Identical and similar amino acids are indicated in black and gray boxes, respectively. Substituted amino acids in the three *htb1* mutants are indicated by arrows (see text). The α-helices are labeled as α1, α2, α3 and αC, whereas L1 and L2 represent the DNA binding loops. (**D**, **E**) The nucleosome structure (D, front view; E, side view; White *et al*, 2001) is depicted with the positions of altered amino acids. The atomic coordinates file (ID; 1ID3) was obtained from Brookhaven Protein Databank (PDB) and visualized with VMD (version 1.8.3). The DNA phosphodiester backbone is shown in gray. The octamer histone chains are schematized by the helical rods and the interhelical loops. Histone H2B subunits are indicated in red. The asterisks indicate the position of K that is associated with monoubiquitin. (**F**) The 3D structure of ubiquitin (PDB ID; 1UBQ) (Vijay-Kumar *et al*, 1987).

S. pombe has the sole gene of H2B, but the two H2A and three paired H3–H4 genes are present in the genome (Matsumoto and Yanagida, 1985); one may expect that only *htb1*$^+$ can generate *ts* mutations.

To determine whether the *ts* mutations actually resided in the *htb1* locus, an integration vector pYC11 carrying the *htb1*$^+$ gene and the *Saccharomyces cerevisiae LEU2* was chromosomally integrated in the *leu1* mutant strain by homologous recombination (because of the low sequence homology between *LEU2* and *leu1*$^+$, homologous integration occurred at the *htb1*$^+$ locus). The resulting Leu$^+$ integrant strain was crossed with *ts* mutants, and tetrad dissection was performed. The Ts$^-$ and Leu$^+$ phenotypes were tightly linked. With the finding that pH2B, but not pH2A, suppressed the *ts* phenotype (Figure 1A), we concluded that the *ts* mutants were derived from the *htb1* locus.

After several rounds of crossing with the wild-type strain for removing extra silent mutations, if any, the *ts* phenotypes of three *ts* strains (*htb1-72*, *-223*, *-442*) at 36°C were characterized. The Ts$^+$ and Ts$^-$ phenotypes were segregated 2:2 for the strains 72 and 223, but not for *htb1-442*. The 442 strain appeared to contain a leaky *ts* and an additional silent mutation (data not shown). We hence employed mostly the two strains *72* and *223* for subsequent physiological experiments. In Figure 1B, the failure of *htb1-72* and *htb1-223* to form colonies on the complete YPD plate at 36°C is shown. The strain *htb1-72* showed the *ts* phenotype severer than *htb1-223* as it did not form colonies at 33°C.

Mutation sites are located in the distinct, but in the conserved and non-helical regions

Mutant genes of histone H2B were obtained from the isolated *ts* strains by the PCR method, and their nucleotide sequences were determined. It was thus established that single-nucleotide substitutions existed for each of the three *htb1* mutant strains. For *htb1-72*, only the 52nd amino-acid residue showed the nucleotide change from GGT to GAT in comparison with the wild-type sequence. For *htb1-223*, the 102nd residue was altered from CCC to CTC. The resulting amino-acid substitutions in *htb1-72* and *htb1-223*, respectively, were

^{52}Gly to Asp (G52D) and ^{102}Pro to Leu (P102L). The *442* segregant that showed the weak *ts* phenotype contained a nucleotide change in the 34th residue (from GAA to AAA), causing the change from Glu to Lys (E34K). These three mutations occurred at the highly conserved residues in histone H2B. The amino acids of the mutation sites were conserved between fission yeast (*Pombe*) and human histone H2B, as shown in Figure 1C.

One of them (*72*) resides in the middle of histone fold, α1–L1–α2–L2–α3, whereas the location of the two others (*223* and *442*) is not within but nearby the histone fold. Residue G52D (72) is positioned in the loop L1 that exists between α1 and α2 helices (Figure 1C). L1 and L2 are the sites to be bound to DNA. In contrast, the P102L residue (223) locates in the short linker between the two helices, α3 and the αC extension. The long αC extension is unique to H2B, and defines the outer limit of the protein surface of nucleosome core particle. P102L is thus close in contact with H2Aα2 by extensive hydrophobic interaction (Luger *et al*, 1997). The E34K (*442*) leaky mutation is in the conserved, amino-terminal tail that is connected to the amino-terminal edge of α1 helix. The physical locations of mutant residues are indicated by the thick arrows in Figure 1D (front view) and Figure 1E (side view) in the nucleosome core structure determined by crystallography (Luger *et al*, 1997; White *et al*, 2001; Richmond and Davey, 2003). The thin arrows with asterisk represent the K119 site to bind to monoubiquitin (Figure 1E and F). The *ts* mutations identified in this study are thus all located in the conserved and non-helical regions. The G52D substitution is in contact with the minor groove of DNA, whereas P102L is in the central region of the histone octamer in the front view (Figure 1D) and in the middle of the outer sides in the side view (Figure 1E). P102L hence interacts with the histone H2A in the same nucleosome, or also with the histones of adjacent nucleosomes (Schalch *et al*, 2005). The E34K substitution is close in contact with DNA.

Missegregation and chromatin shrinkage occur in htb1 mutants

We investigated whether these *htb1* mutations affected the cell division cycle of *S. pombe*. Exponentially growing cultures of wild-type, *htb1-72* and *htb1-223* strains at 26°C in the complete YPD were shifted to 36°C for 12 h. Cells were scored for viability and observed by DAPI staining after glutaraldehyde fixation. Interestingly, *htb1-223,* but not *htb1-72,* showed frequent unequal nuclear division after 8 h at 36°C (arrowheads in Figure 2A, lower right panel), the characteristic phenotype seen in the centromere/kinetochore protein mutants (Takahashi *et al*, 1994, 2000; Saitoh *et al*, 1997; Goshima *et al*, 1999; Hayashi *et al*, 2004). Quantitative data (Figure 2B, red line with rectangles in the middle panel) showed that the frequency of cells with unequal daughter

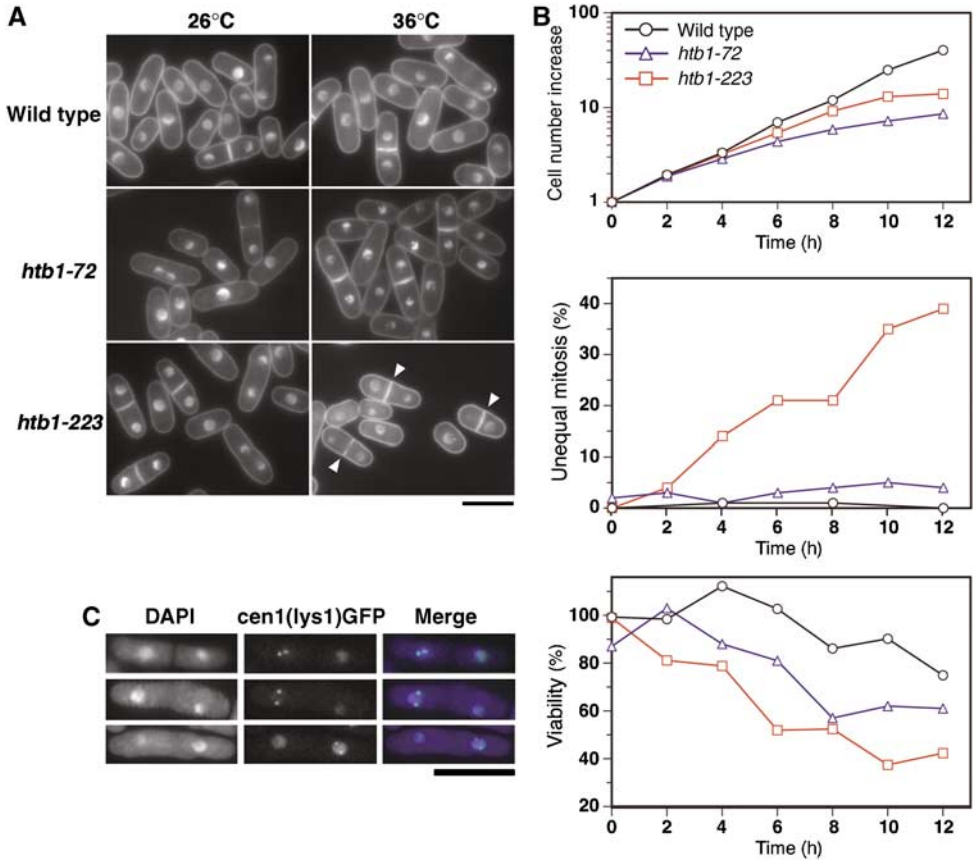

Figure 2 Cellular phenotypes of histone H2B mutants *htb1-72* and *htb1-223*. Asynchronously growing *htb1* mutant cells in YPD medium were shifted to 36°C for 0–12 h. (**A**) Mutant cells cultured at 26°C (left panels) or 36°C for 8 or 12 h (right panels) were stained by DAPI. Upper panels, wild type; middle panels, *htb1-72*; lower panels, *htb1-223*. Arrowheads indicate binucleate cells displaying unequal nuclear division. Bar, 10 μm. (**B**) Top, cell number increase; middle, the frequencies of unequal nuclear division; bottom, cell viability. (**C**) Unequal chromosome segregation was examined by the *cen1*(*lys1*)-GFP method (see text). Three examples of *htb1-223* mutant cells cultured at 36°C for 10 h displaying unequal segregation of *cen1*(*lys1*)-GFP signals are shown. Bar, 10 μm.

nuclei increased after 4 h at 36°C in coincidence with the gradual decrease of cell viability (bottom panel), and reached 38% of binucleated cells. Typical centromere/kinetochore protein mutants *mis6* and *mis12* produced ~80% unequal nuclei in binucleate cells so that the unequal segregation phenotype of *htb1-223* was not severe as *mis6* and *mis12*. The unequal nuclear division phenotype was scarce (a few %) in *htb1-72*. Instead, the nuclear chromatin observed by DAPI staining appeared to be shrunk (12 h; Figure 2A, middle right panel). Cell viability of *htb1-72* decreased at the time of nuclear chromatin shrinkage. The gross chromatin organization in *htb1-72* appeared to be altered. Additionally, the thick septa indicative of cytokinesis delay were observed in *htb1-72*.

To confirm that the unequal nuclear division phenotype of *htb1-223* was due to chromosome missegregation, the *cen1*-GFP method (Nabeshima *et al*, 1998) was employed. After 10 h at 36°C, 25% of the binucleate *htb1-223* cells (50/204) exhibited unequal nuclear division. As shown in Figure 2C, the *cen1*-GFP signals failed to segregate in these cells. Missegregation of *cen1*-GFP signals was observed in 22% (11/50) of cells showing unequal nuclear division. We thus concluded that the unequal nuclear division phenotype in *htb1-223* mutant was owing to chromosome missegregation.

Histone H2B mutants were sensitive to a protein synthesis inhibitor

To understand the causes for the histone H2B mutants to produce distinct phenotypes, we examined whether these mutants might be differentially sensitive to drugs and irradiation. Effects of hydroxyurea (DNA replication inhibitor) and UV irradiation were tested, but their sensitivities were similar to that of wild type (data not shown). Cycloheximide (Cyh, a protein synthesis inhibitor), however, showed different sensitivities as shown in Figure 3A. At 30 and 33°C (semi-

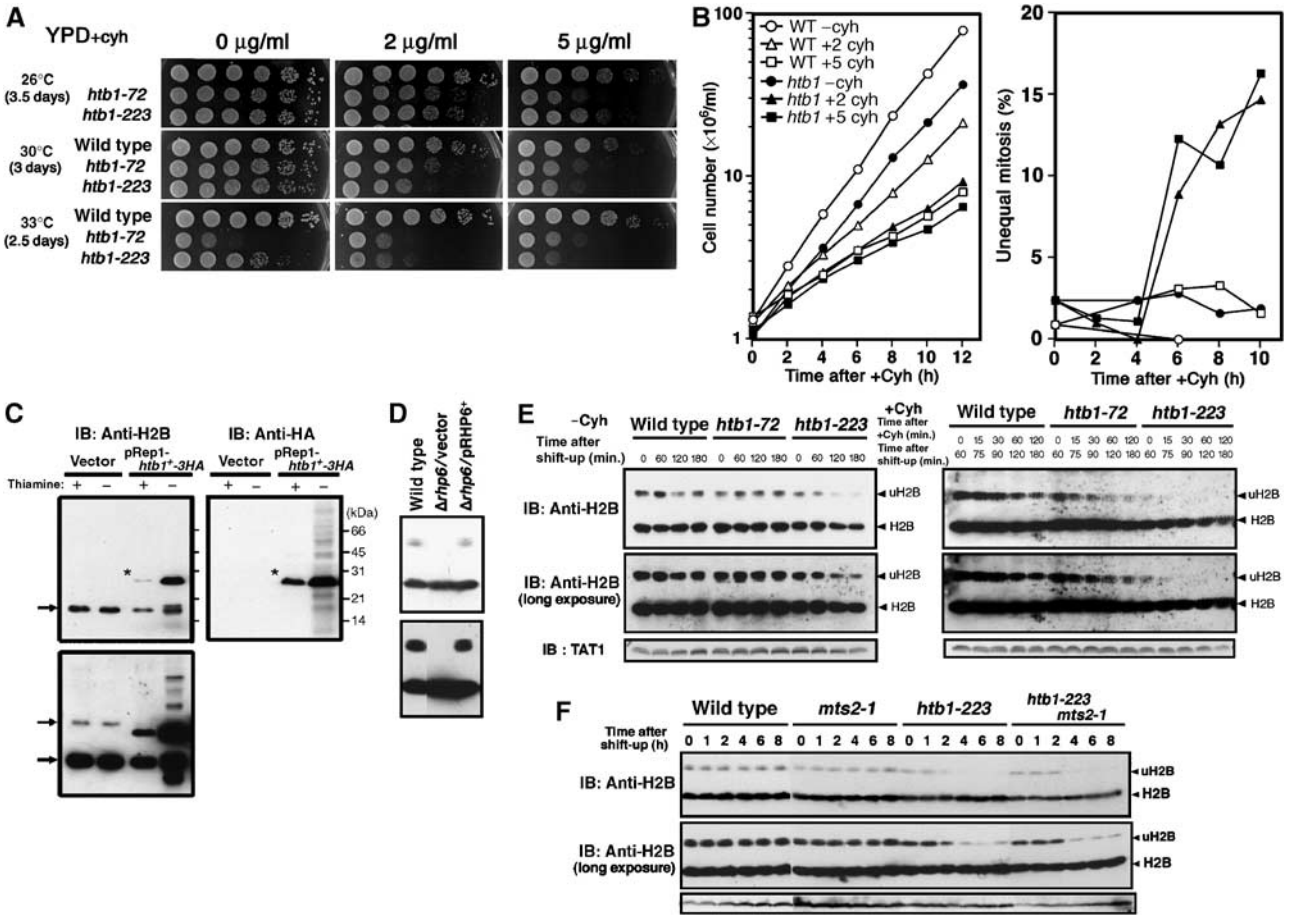

Figure 3 Cyh sensitivity and turnover of Rhp6-dependent ubiquitination of H2B in *htb1* mutants. (**A**) The *htb1* mutants are hypersensitive to Cyh, a protein synthesis inhibitor. Both *htb1-72* and *htb1-223* were slower in growth than wild type in the presence of Cyh. Cells were serially diluted (1:5) and spotted onto the YPD plates containing Cyh (0, 2 and 5 μg/ml). The highest-density spots contained 5×10^4 cells. (**B**) The cell number increase (left panel) and the frequencies of unequal nuclear division (right) are shown for wild type (open) and *htb1-223* (closed) in the absence (circles) or presence (rectangles, triangles) of Cyh at 33°C. (**C**) Immunoblot patterns using polyclonal antibodies against histone H2B (anti-H2B) and monoclonal antibodies against HA (anti-HA). Extracts of cells expressing endogenous H2B (Rep1 vector) and ectopically expressed H2B tagged with HA (pRep1-*htb1*HA) in the presence of thiamine (promoter off) and absence of thiamine (14 h after removal of thiamine; promoter on) were used for immunoblot. The 17 kDa H2B band and the 24–25 kDa uH2B bands (indicated by the arrows) were detected in cells carrying vector. In cells carrying p*Rep1-htb1*HA, additional bands for H2B-3HA (asterisks) were detected by anti-H2B and anti-HA antibodies. (**D**) Immunoblot was performed for extracts of wild type, Δ*rhp6* carrying vector or plasmid pRHP6. The presumed monoubiquitinated H2B band was missing in Δ*rhp6*. (**E**) Wild type, *htb1-72* and *htb1-223* were cultured in the absence (−) or presence of (+) of Cyh (100 μg/ml) at 36°C for 0–180 min. In the case of +Cyh, strains were first cultured at 36°C for 60 min and then followed by the addition of Cyh. Immunoblot patterns by short and long exposure are shown. The positions for H2B and uH2B are indicated by arrowheads. (**F**) Wild type, *mts2-1*, *htb1-223* and the double mutant *mts2-1 htb1-223* were cultured first at 26°C, and then shifted to 36°C for 8 h. Immunoblot patterns using anti-H2B antibodies indicated that the level of decrease of uH2B was not arrested in the proteasome mutant *mts2-1* background.

restrictive temperature), both *htb1-72* and *htb1-223* were sensitive to Cyh. At 30°C, *htb1-223* was more sensitive than *htb1-72*. Introducing pH2B plasmid into the mutants restored the hypersensitivity (data not shown), indicating that the *htb1* mutations caused both *ts* and Cyh phenotypes. The addition of Cyh thus produced the synthetic lethal effect on *htb1* mutations.

We then tested whether Cyh affected the cellular phenotypes of the *htb1-223* mutant at 33°C, the semi-restrictive temperature. To this end, the culture of *htb1-223* grown at 26°C was shifted to 33°C for 2 h in the absence of Cyh followed by the addition of Cyh (2 and 5 μg/ml) for the continued culture at 33°C for 12 h (Figure 3B). For control, wild type without or with Cyh (5 μg/ml) was tested. In the absence of Cyh, the frequency of unequal nuclear division was negligible in *htb1-223* at 33°C. In the presence of Cyh, however, the cell number increase (left panel) was considerably retarded and the frequency of unequal nuclear division (right panel) strikingly increased after 4 h. These results suggested that the level of functional H2B protein might decrease in the presence of Cyh in *htb1-223* mutant at the semi-restrictive temperature (see below).

Rhp6-mediated monoubiquitination of H2B

The above results suggested that mutant histone H2B might be unstable or faster in turnover than that of wild-type histone H2B. The inhibition of protein synthesis might reduce the level of mutant histone H2B. To test this hypothesis, polyclonal antibodies against a 16 amino-acid peptide of the amino-terminal tail sequence SAAEKKPASKAPAGKA of *S. pombe* histone H2B were raised. Immunoblot of cell extracts were carried out using affinity-purified anti-H2B antibodies. An intense ~17 kDa band (corresponding to histone H2B) was seen in wild-type cells carrying vector plasmid pREP1 (Figure 3C, left). A weak ~25 kDa band (indicated by the arrows) was observed in the long exposed immunoblot patterns. This 25 kDa band corresponds to monoubiquitinated histone H2B (designated uH2B; see below).

The assignment of the bands was confirmed using extracts of cells that expressed the HA-tagged histone H2B under the control of the inducible *nmt1* promoter (Figure 3C). Antibodies against H2B (left panel) and against HA (right panel) were used to detect HA-tagged H2B that was overproduced in the absence of thiamine (promoter, on) for 14 h after the removal of thiamine. The HA-tagged H2B band (indicated by asterisks) was dramatically increased in the absence of thiamine. Polyclonal antibodies against H2B thus detected both endogenous and ectopically expressed H2B.

The 25 kDa upper H2B band was produced in an Rhp6-dependent manner. As shown in Figure 3D, the upper band disappeared in the deletion mutant Δ*rhp6* (Kitamura *et al*, 2001). This band was restored in Δ*rhp6* carrying plasmid pRHP6 (constructed by PCR method in this study). Rhp6 is a homolog of budding yeast Rad6, a ubiquitin conjugating enzyme, which is known to be responsible for monoubiquitination of histone H2B (Robzyk *et al*, 2000). We hence supposed that the 25 kDa band was an Rhp6-mediated monoubiquitinated band. The band intensity of uH2B in the absence of Cyh was approximately 10% of total cellular histone H2B in wild type.

Monoubiquitinated H2B-223 mutant protein is unstable

We then tested whether mutant H2B was less stable than wild type in the presence or absence of Cyh. Cyh (100 μg/ml) was added to the cultures of wild type, *htb1-72* and *htb1-223*, 60 min after the shift to 36°C, and cell extracts were prepared. Immunoblot patterns of wild-type and mutant extracts using antibodies against histone H2B are shown in Figure 3E. Although the levels of H2B remained high and did not alter significantly, the uH2B level in *htb1-223* mutant was already low before the shift (roughly 50% compared with that in wild-type cells), and decreased after the shift to 36°C in the absence of Cyh. In the presence of Cyh, the level of uH2B-223 rapidly decreased. The levels of wild-type uH2B and other mutant uH2B-72 also decreased in the presence of Cyh.

The quantitative densitometric analyses of immunoblot patterns indicated that the half-life of uH2B-223 in the presence of Cyh at 36°C was only 15 min, whereas those in wild type and *htb1-72* were 88 and 86 min, respectively. In the absence of Cyh, mutant H2B-223 became unstable by the temperature shift to 36°C, and the apparent half-life of uH2B-223 was 92 min. The level of H2B in wild type and *htb1-72* did not alter in the absence of Cyh. We therefore concluded that the half-life of uH2B was specifically short in *htb1-223*.

Instability of uH2B in htb1-223 is not due to 26S proteasome-dependent proteolysis

A question was raised whether instability of ubiquitinated H2B was due to proteolysis. Immunoblot of H2B protein was carried out for extracts in a proteasome mutant *mts2-1* and the double mutant *mts2-1 htb1-223*. As shown in Figure 3F, the level of uH2B was not affected at all in the absence of 26S proteasome function for wild-type H2B, but mutant H2B-223 protein destruction seemed to be slightly suppressed so that mutant uH2B might go through the proteasome for degradation. However, the decay in the level of uH2B might be principally owing to deubiquitination rather than 26S-dependent proteolysis. In any case, uH2B became highly dynamic in *htb1-223* cells in the presence of Cyh so that chromatin would be strongly altered if uH2B was indispensable.

Ubiquitination-deficient H2B does not support cell viability

To investigate whether instability of uH2B has any physiological consequence, we constructed a plasmid containing *htb1-K119R* mutant gene (pH2B-K119R) that had a lysine-to-arginine substitution at the conserved monoubiquitination site K119 of histone H2B to R by site-directed mutagenesis. Plasmid pH2B-K119R tagged with FLAG and under the inducible promoter *nmt1* failed to produce the normal band of uH2B (Supplementary Figure 1). We first tested whether high-copy plasmid pH2B-K119R could complement the *ts* phenotype of *htb1* mutants. As shown in Figure 4A, pH2B-K119R suppressed neither the *ts* phenotype of *htb1-72* nor *htb1-223*. Secondly, we examined whether *htb1-223* mutant carrying plasmid pH2B-K119R displayed the missegregation phenotype at 36°C. Although the appearance was delayed, the missegregation phenotype was still observed (closed diamonds in the middle panel in Figure 4B). In addition, the septation index increased, indicating that cytokinesis was delayed, resembling the phenotype of *htb1-72*. In control *htb1-223* cells carrying wild-type plasmid pH2B, no missegregation phenotype was observed.

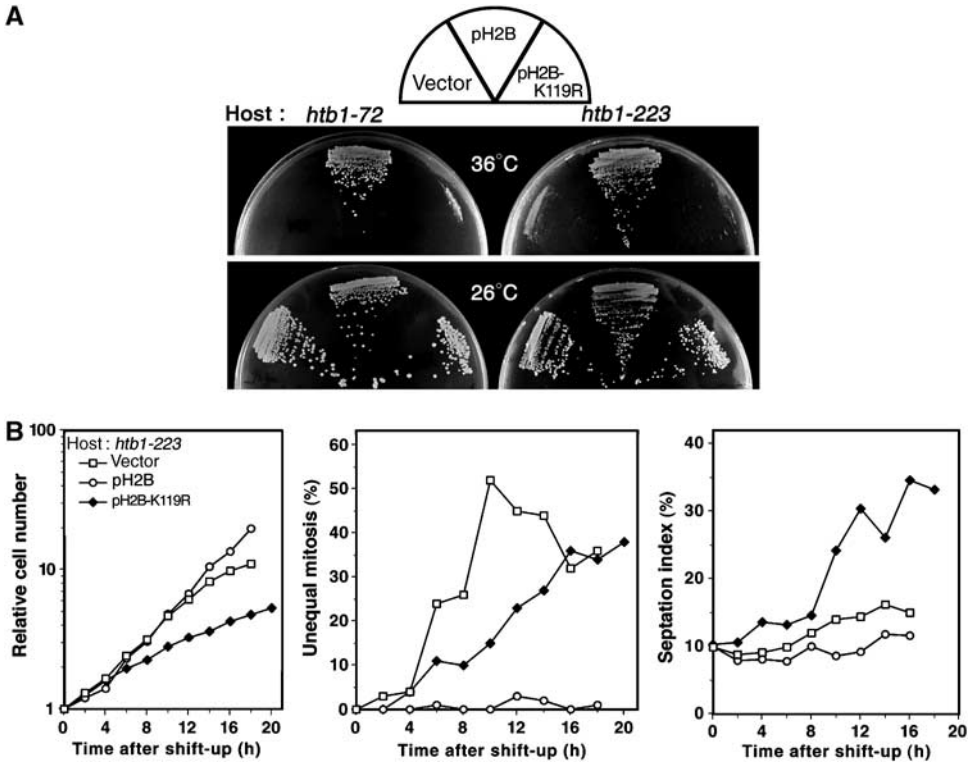

Figure 4 H2B K119R mutant substituted at monoubiquitination site fails to suppress the phenotype of *htb1* mutant. (**A**) Plasmid carrying the *htb1-K119R* gene failed to suppress the *ts* phenotype of *htb1-72* and *htb1-223* mutants. (**B**) The cultures of *htb1-223* mutant carrying vector, pH2B, or pH2B-K119R were asynchronously grown in the EMM2 medium and shifted to 36°C. The cell number increase (left panel), the frequencies of unequal nuclear division phenotype (middle) and the septation index (right) after the shift-up are shown.

CENP-A localization was partly diminished in htb1-223

To examine whether Cnp1, the centromere-specific histone H3 variant CENP-A in fission yeast (Takahashi *et al*, 2000), could be normally localized to the centromere in *htb1-223* mutant, the *cnp1*$^+$ gene was tagged with GFP and integrated onto the chromosome and expressed under the native promoter. Cnp1-GFP signal was observed after methanol fixation. In control *htb1*$^+$ cells, Cnp1-GFP signals were observed as dots signals in nuclei throughout the cell cycle. After shifting-up to 36°C, the frequencies of cells with dots signals in *htb1*$^+$ were 83% (0 h), 76% (4 h) and 76% (8 h) (Figure 5A, bottom panel). However, in *htb1-223* cells cultured at 36°C for 8 h, the frequencies of Cnp1-GFP signals were significantly diminished from 82% at 26°C (0 h) to 53% at 36°C (6 h). Examples of the dot and dispersed signals of Cnp1-GFP are shown in the upper panels of Figure 5A. Quantitative data are indicated in the lower panel. The blue portions represent the fractions of cells that displayed the dispersed Cnp1-GFP signals. The frequencies of centromeric Cnp1-GFP in *htb1-72* cells, however, are similar as those in *htb1*$^+$. These results suggested that Cnp1 was not properly loaded onto centromere in *htb1-223* or that centromeric chromatin architecture was structurally spread whereas Cnp1 binding to centromeres remained. We examined whether Rhp6 has any influence over Cnp1 localization, and found that Cnp1 localization was normal in Δ*rhp6* deletion mutant cells (data not shown), suggesting that monoubiquitinated H2B did not seem to be implicated in Cnp1 localization.

To further substantiate the above localization result, chromatin immunoprecipitation (CHIP) was performed under the *htb1* mutant background. The *cnp1*$^+$ gene was tagged with HA and integrated onto the chromosome under the native promoter (Takahashi *et al*, 2000). Cnp1-HA was immunoprecipitated after formaldehyde fixation. The levels of PCR signals in the *htb1-223* mutant background were estimated, using the central centromere primers (*cnt* and *imr*). As shown in Figure 5B, the CHIP patterns (lower left) and their quantitative estimations (lower right) indicated that the levels of the central centromere sequences bound to Cnp1 were reduced after the shift-up to 37°C. Wild-type and *mis6-302* are also shown as a control: it is known that Cnp1 centromere localization is greatly reduced in *mis6-302* (Takahashi *et al*, 2000). These results supported the possibility that *htb1-223* mutation had an effect on Cnp1 centromere localization, and showed that the degree of association between centromeric DNA and Cnp1 was diminished. The *t*-test was conducted and the *P*-values obtained were 0.024 and 0.013 for *cnt* and *imr*, respectively. A possibility was raised that, if nucleosome density was altered by the H2B mutation, then the measurements of nucleosome modifications and variants are not informative without correction for nucleosome content. We therefore performed CHIP using anti-H2B antibodies. No significant change in the nucleosome density was found in the centromeric regions (Figure 5B).

Partial disruption of specialized centromere chromatin in htb1-223

The above experiments could not establish that centromeric chromatin was disrupted in *htb1-223* mutant cells. To examine whether centromeric structure was defective in *htb1-223*, we performed a micrococcal nuclease digestion experiment.

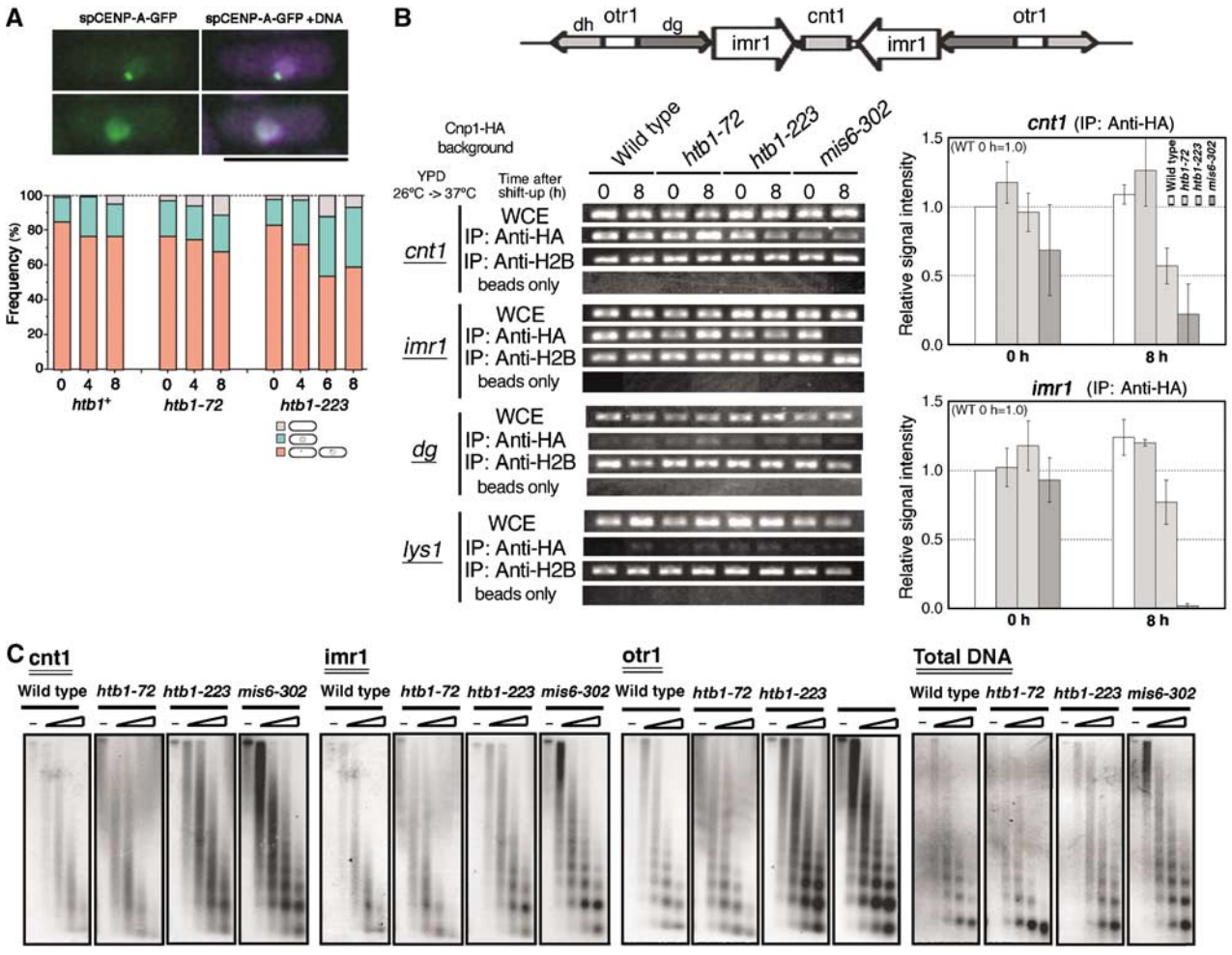

Figure 5 Centromere-specific chromatin structure is partly disrupted in *htb1-223* mutant cells. (**A**) Cnp1-GFP signals (green) were observed in the *htb1* mutant background. DAPI was used to stain DNA (purple). Bar, 10 μm. For quantitative measurements, cells were grouped into three classes based on the localization patterns of Cnp1: the dots signals (orange), the dispersed signal (blue) and no detected signal (gray). (**B**) CHIP experiment was performed using the central centromere probes of *cnt1*, *imr1*, the outer heterochromatic repeat *dg* and pericentric *lys1* (lower left). The organization of *cen1* is schematized (top). Relative signal intensities were determined and quantitative data are shown (lower right, the value for wild type 0 h is 1.0). The amount of *cnt1* and *imr1* DNAs co-precipitated with the Cnp1-HA fusion was reduced in *htb1-223* mutant cells at 37°C (anti-HA for *cnt1* and *imr1*). (**C**) Micrococcal nuclease experiments. Nuclear chromatin were prepared from wild-type, *htb1-72*, *htb1-223* and *mis6-302* cells that were cultured at 37°C for 7 h, and digested with micrococcal nuclease for 0, 1, 2, 4 and 8 min, followed by agarose gel electrophoresis and Southern hybridization using the three centromeric DNA probes *cnt1*, *imr1* and *otr1*. The ethidium bromide staining patterns of the gel are also shown.

When nuclear chromatin of wild-type *S. pombe* is digested with micrococcal nuclease, Southern blot using the probes of inner centromere DNAs displays a specialized chromatin with smeared digestion pattern (Polizzi and Clarke, 1991; Takahashi *et al*, 1992). In *cnp1, mis6* and *mis12* centromere-defective mutants (Saitoh *et al*, 1997; Goshima *et al*, 1999; Takahashi *et al*, 2000), the specialized chromatin was abolished and this was the cause for unequal chromosome segregation. We tested whether the centromere-specific chromatin digestion pattern was impaired in *htb1-223* mutant. As shown in Figure 5C, the smeared patterns were significantly diminished, and the more regular-ladder like patterns were obtained for the *imr* centromere probes in *htb1-223* mutant at 37°C for 7 h (Figure 5C, *imr1*). The smeared pattern was maintained in the *cnt* region, however. The digestion pattern of *htb1-72* was smeared as that in wild type. The pattern for *mis6-302* is also shown as a control of the loss of specialized chromatin. These results showed that the specialized centromere chromatin was disrupted in the *imr* region of *htb1-223* mutant cells. The *imr* regions are inverted repeats that are 100% identical in each centromere and contain a number of tRNA genes (Takahashi *et al*, 1991).

We tested whether Rhp6 has any effect on centromere chromatin. To this end, micrococcal nuclease digestion experiment was carried out for Δ*rhp6* deletion mutant. As shown in Supplementary Figure 2, the smeared digestion patterns were observed in the central centromere chromatin in Δ*rhp6* mutant cells, suggesting that the reduced mono-ubiquitination of H2B did not significantly affect centromere chromatin at the level of micrococcal digestion pattern.

Genetic interactions of htb1-223 with segregation-defective mutants

To identify genetic interactions between *htb1* and various mutations, we constructed the double mutants. The results are shown in Table I. Synthetic growth defects at the permissive temperature were found for the double mutants of *htb1-223* with *cnp1-1*, *mis6-302*, *mis12-537* or *dis1-288*.

Table I Synthetic genetic interactions of *htb1-72* and *htb1-223* mutants with various mitotic, phosphatase, kinase and deacetylase mutants

	htb1-72	htb1-223
cnp1-1	ND	Lethal
mis6-302	No effect	Synthetic growth defect
mis12-537	No effect	Synthetic growth defect
dis1-288	No effect	Synthetic growth defect
dis2-11	Synthetic growth defect	Synthetic growth defect
Δ*pka1*	No effect	Suppression
clr6-1	Synthetic growth defect	Weak synthetic growth defect
cut9-665	No effect	No effect
mts2-1	No effect	No effect

ND, not determined.

These mutants were all defective in centromere/kinetochore functions (Nakaseko *et al*, 1996; Saitoh *et al*, 1997; Nabeshima *et al*, 1998; Goshima *et al*, 1999; Takahashi *et al*, 2000). Such synthetic phenotypes were not observed at all for the double mutants employing the allele of *htb1-72* (Supplementary Figure 3). These results confirmed that centromere/kinetochore functions were defective *in htb1-223*.

For the double mutants using *dis2-11* (defective in type 1 protein phosphatase) and *clr6-1* (histone deacetylase, HDAC) (Ohkura *et al*, 1989; Grewal *et al*, 1998), both *htb1-223* and *htb1-72* showed the same synthetic effects, and for *pka1* deletion mutants (cAMP-dependent kinase) (Yamashita *et al*, 1996) suppressed the *ts* phenotype of *htb1-223*. It may not be surprising for H2B to interact with PP1, PKA and HDAC as H2B is known to have the sites for phosphorylation and acetylation in the amino-terminal tail. The above results suggest that deacetylated and dephosphorylated H2B is appropriate for the central centromere chromatin, consistent with our current view for the assembly mechanism of central centromeric architecture (Hayashi *et al*, 2004). The phosphorylation site in the tail has the PKA consensus sequence. Opposite effects of Dis2 (PP1) and PKA on both *htb1* mutants are consistent with a hypothesis that they may competitively act on the same phosphorylation site.

Chromatin silencing diminished in htb1 mutants

We examined whether transcriptional silencing was normal in the *htb1-72* and *htb1-223* mutant background. To this end, the *ura4*$^+$ reporter gene chromosomally inserted in the heterochromatin regions was employed (Ekwall *et al*, 1996, 1999). In *S. pombe*, centromere, telomere and the mating-type locus are heterochromatic regions, and the common DNA sequences are present. Centromere consists of the central core domain (*cnt*), the inverted repeats domain flanking the central core (*imr*) and the outer heterochromatic repeats domain (*otr*), as shown in Figure 5B. To examine gene expression in *htb1* mutants, expression of the inserted *ura4*$^+$ was assayed by growth on non-selective (N/S) and counterselective (5-fluoroorotic acid (5-FOA), which inhibits the growth of Ura$^+$-expressing cells) media. As shown in Figure 6A (top panel, 30°C in the YPD medium), derepression of *ura4*$^+$ occurred in the whole centromeres (*cnt1*, *otr1*) and the mating-type locus (*mat3*) in the *htb1-72* mutant background. However, in the *htb1-223* background, silencing was maintained in these *ura4*$^+$ inserted cells as in wild-type cells. The control of dicer deletion (Δ*dcr1*; Volpe *et al*, 2003) that is desilenced is also shown. These results demonstrated that transcriptional silencing was generally abolished in *htb1-72* but not in *htb1-223* under this experimental condition (YPD, 30°C). When the synthetic medium EMM2 was used at 33°C for assaying the silencing in the *htb1-223* background, it became possible to detect desilencing in the *cnt1* but not in the *otr* region (Figure 6A, bottom panel).

Mutations such as Δ*swi6* that disrupt the formation of outer centromeric silent chromatin are known to cause lagging chromosomes in anaphase at low temperature (Ekwall *et al*, 1995, 1996). We examined whether the same was true for *htb1-72* mutant cells by immunofluorescence microscopy using DNA and tubulin staining (Figure 6B). Quantitative data are indicated in the table. The *htb1-72* cells were found to display a high incidence of lagging chromosomes on anaphase spindle (27%, $n=100$) at a low temperature, 18°C. On the other hand, *htb1-223* cells showed much lower incidence of lagging chromosomes (7%, $n=100$) at 18°C. In wild-type cells, lagging chromosomes were scarce (1%, $n=100$) at 18°C. Although lagging chromosomes were observed in both Δ*swi6* and *htb1-72* mutants, underlying defects might greatly differ, as *htb1-72* was not sensitive to TBZ, a tubulin poison (Supplementary Figure 4). The cause of lagging chromosome in *htb1-72* might be owing to chromatin defect rather than spindle–chromosome interaction defect.

Altered histone modifications in the centromere chromatin of htb1 mutant

To further substantiate alterations of histone modifications, we performed the CHIP experiments for *htb1* mutants cultured at the restrictive temperature for 8 h, using the central centromere probe (*cnt*) and a pericentric probe for the regular gene *lys1*. Results using antibodies against acetylated histones H3 (AcH3) and H4 (AcH4), and Lys 4 di- or trimethylated H3 (MeH3K4) under the *htb1* mutant background with the control of wild-type and *mis16-53* mutant are shown in Figure 6C. It was previously demonstrated that histone H4 was hyperacetylated in control *mis16* mutant, specifically in the central centromere regions (Hayashi *et al*, 2004). An extensive study using the CHIP-on-CHIP method showed that Lys 4-methylated histone H3 was present in the central centromere regions (Cam *et al*, 2005). In this experiment, it was found that methylation of histone H3 in the central centromere also increased in *mis16*. Both effects were limited in the central centromere regions in *mis16* mutant. In the *htb1-72* mutant background, however, such central centromere-specific hyperacetylation or hypermethylation was not found in comparison with the wild-type control. In *htb1-223*, however, acetylation and methylation slightly increased, but the degree of increase was much less than the case of *mis16* centromere mutant cells. These CHIP experiments were performed twice, producing reproducible results, and for Figure 6C, the *P*-values obtained by the *t*-test for AcH4, AcH3 and MeH3 were 0.076, 0.100 and 0.022, respectively. A question was raised whether the nucleosome density might be altered by the H2B mutants. If so, the measurements of nucleosome modifications and variants require correction for nucleosome content. The H2B levels were thus examined by immunoblot using antibodies against H2B (Figure 6D), and it was found that there was no significant variation in the H2B contents among the wild type and mutants.

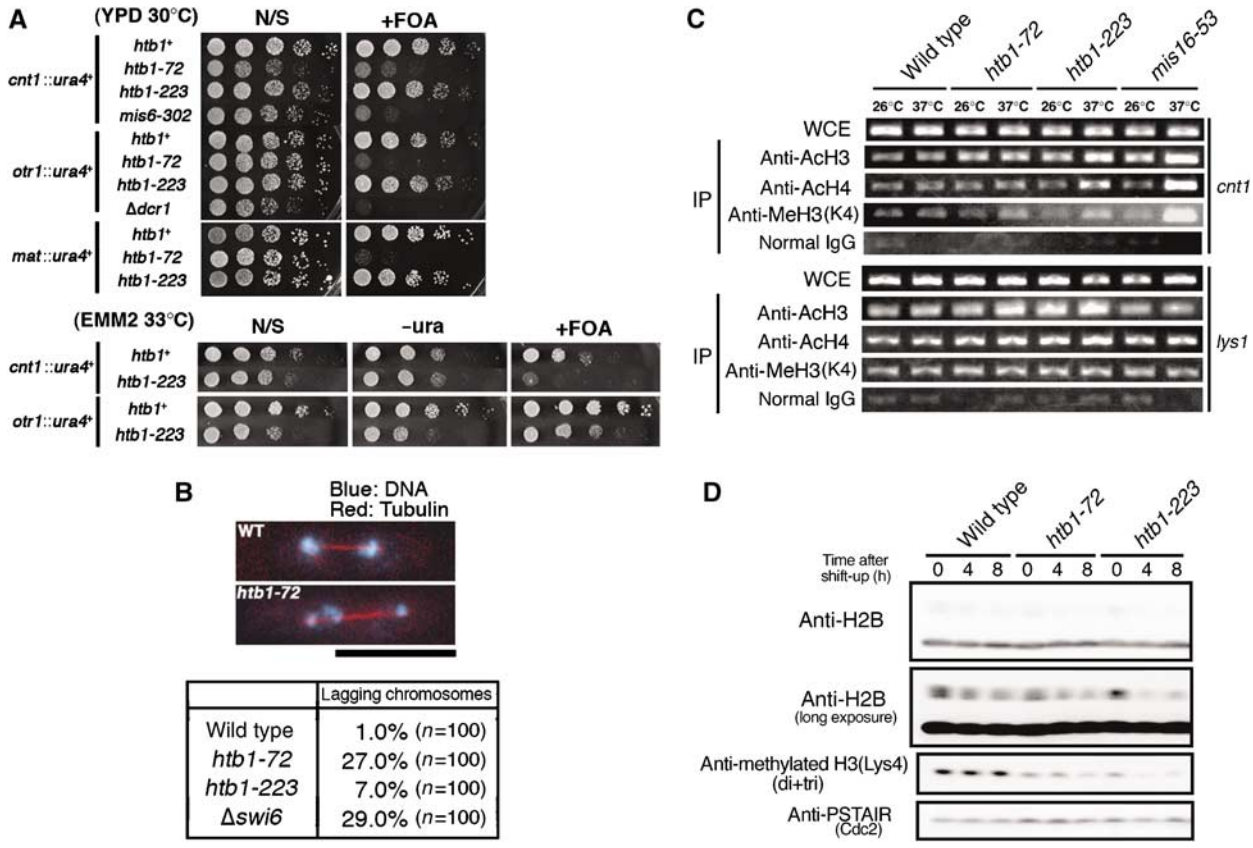

Figure 6 Effect of *htb1* mutations on silencing of the inserted *ura4*$^+$ marker gene and histone modification patterns in the centromere region. The *ura4*$^+$ insertion sites within *cen1*: *otr1R*::*ura4*$^+$ and *cnt1*::*ura4*$^+$ are indicated by the short bar in the top panel of Figure 5B. (**A**) Cells were serially diluted (1:5) and spotted onto the YPD plates: non-selective (N/S) or containing 5-FOA. They were incubated at 30°C for 3 days, or they were spotted onto the EMM2 plates: nonselective (N/S), lacking uracil (−URA) or containing 5-FOA. The highest-density spots contained 1×10^4 cells. (**B**) Lagging chromosomes observed in anaphase of *htb1-72* cells at 18°C. (**C**) Histone acetylation and methylation patterns in the centromere region were altered in *htb1-223* mutant. The levels of histone H3 and H4 acetylation and methylation in the centromeric regions were examined by CHIP using antibodies against acetylated H3 and H4. Anti-AcH4 is against acetylated K5, K8, K12, K16 in H4, whereas anti-AcH3 is against acetylated K9 and K14 in H3. Antibodies against dimethylated K4 in H3 were also used. The centromere probes used were central *cnt1*, although pericentric probe *lys1* was also used. Indicated strains were cultured at the restrictive temperature (37°C) for 0 or 8 h. (**D**) The levels of histone H2B and (di- or tri-) methylated histone H3 (Lys4) in *htb1* mutant cells were examined by immunoblotting. The levels of Lys4 (di- or tri-) methylated histone H3 were diminished in *htb1* mutants, particularly in *htb1-223* cells.

Discussion

In this study, we report pleiotropic phenotypes of three *htb1* mutants, which contained amino-acid substitutions at non-helical residues in the highly conserved inner structure of histone H2B. Each mutant showed quite distinct, characteristic cellular phenotypes that include Cyh hypersensitivity, defective monoubiquitination, gene silencing, centromere chromatin and chromosome segregation. One strain (E34K) was only slightly slow in the cell number increase (data not shown), whereas two other strains (G52D and P102L) showed the clear *ts* phenotypes. Isolation of these mutants appeared to be possible because of the sole H2B gene. The same situation may be applied if three other histone genes, H2A, H3 and H4, will be disrupted and the single remaining histone subtype gene is mutagenized randomly or in a site-directed manner. It was once thought that substitution-type *ts* mutants might be scarce for the histone genes, as the sequence was extremely conserved during evolution. This seemed to be, however, a misconception. In this study, three H2B substitution mutants could be obtained by screening only ~500 *ts* strains. Further, the substitution of conserved E34 residue to K showed little phenotype. Curiously, all the mutated residues were located in the non-helical regions, probably because the structurally flexible loop and the linker regions between helices might be able to produce conditionally altered conformations at different temperatures. These mutants will provide a unique opportunity to experimentally dissect the roles of H2B in the formation of heterochromatin and complex centromeres, and the regulation of gene silencing by siRNA in *S. pombe*.

The *htb1-72* mutation was substituted (G52D) in the DNA-contacting loop L1 of histone fold, and became lethal after 8 h at 36°C. In these mutant cells, broad gene desilencing occurred in the heterochromatin of centromere and the mating-type locus. Overall chromatin structure including the heterochromatin regions might be affected. In fact, the interphase nuclear chromatin stained by DAPI was clearly shrunk (compacted) after 12 h. Although no obvious mitotic defect was observed at the restrictive temperature (36°C), lagging chromosomes were abundantly seen in *htb1-72* at a rather low temperature (18°C) after 12 h. As *htb1-72* differed from Δ*swi6* in its insensitive nature to TBZ, further investigation is needed to clarify the nature of lagging chromosomes.

Centromere architecture rather than spindle–kinetochore interaction might be defective in *htb1-72* mutant at a low temperature, and lagging chromosomes observed were owing to the defect in centromere chromatin itself.

The *htb1-223* mutation is substituted (P102L) in the short linker region between α3 and αC helices. The αC extension is specific to H2B and not an element of the histone fold. This extension forms a part of the outer protein surface that also contain antiparallel H2B α3 helix and H2A α2 helix, bound by the strong hydrophobic interaction (Luger *et al*, 1997). An attractive hypothesis is that *htb1-223* affects the chromatin fiber formation by altering the interface interactions between the adjacent nucleosomes. This is consistent with the crystal structure of a tetra-nucleosome recently solved (Schalch *et al*, 2005). It reveals that linker DNA zigzags back and forth between two stacks of nucleosome cores and that H2B αC is present in the interface between two adjacent nucleosome cores in the chromatin fiber models. This interface might be structurally defective in *htb1-223* mutant so that the central centromeric chromatin essential for equal chromosome segregation might be disrupted. Additionally, monoubiquitinated H2B in *htb1-223* might become accessible to deubiquitinase or protease. Alternatively, monoubiquitination of H2B might become inefficient in *htb1-223* owing to the inaccessibility of ubiquitin conjugating or ligating enzyme.

Two striking phenotypes, frequent unequal chromosome segregation and short-lived uH2B (half-life, 15 min), were found in *htb1-223*. A specific higher-order chromatin fiber in the central centromere region might be impaired in mutant cells. We suspect that monoubiquitin bound to mutant H2B is either inefficiently ligated, rapidly deubiquitinated or degraded by non-proteasomal protease. It is tempting to speculate that centromere/kinetochore function requires proper monoubiquitination and long half-life of uH2B. However, our results do not support such hypothesis. The centromere location of Cnp1 and the micrococcal nuclease digestion patterns appear to be normal in Δ*rhp6* deletion that is responsible for monoubiquitination. uH2B itself may be unstable in these mutant cells. The defect in Cnp1 loading is most likely not due to defective monoubiquitination of H2B but solely due to P102L mutation. In consistence with the results of synthetic genetic interactions, centromeric CENP-A localization determined by Cnp1-GFP and CHIP was diminished in *htb1-223* cells at restrictive temperature (Figure 5A and B). Further, the innermost repeat (*imr*) regions appeared to lose the specialized chromatin detected by micrococcal nuclease digestion (Figure 5C). Taken together, chromatin in the central centromere was functionally and structurally impaired in *htb1-223*, probably owing to the change in protein conformation of mutant H2B protein.

Certain phenotypes of the H2B mutants isolated in this study might be caused by general defects in transcription, so that the expression of other genes involved in these processes are affected, thus causing the observed phenotypes. We measured the level of total RNAs before and after (8 h, 36°C) the temperature shift of H2B mutants, and found that the levels did not alter significantly (data not shown), indicating the lack of great reduction or increase of transcription in these mutants. In *htb1-223*, the smear-like pattern is changed to a regular ladder at *imr1*, but only a little change is observed at *cnt1*. While Cnp1 levels are generally supposed to correlate with smear-like digestion patterns, Cnp1 levels are more reduced at *cnt1* than at *imr1* in *htb1-223*. We have no satisfactory explanation for this apparent discrepancy. The *imr* regions contain a large number of tRNA genes, but the *cnt* regions do not. Recently, these tRNA genes were reported to play a role in chromatin boundary (Scott *et al*, 2006). The changes in the *imr* chromatin structure due to a slight decrease of Cnp1 enrichment might be amplified to a significant change in the micrococcal nuclease digestion pattern. Alternatively, the chromatin properties detected by the digestion and Cnp1 CHIP are different, so that an unknown defect in H2B mutant protein might cause these two phenotypes.

In the budding yeast *S. cerevisiae*, the substitutions in histone H4 caused the *ts* phenotype defective in mitotic chromosome transmission (Smith *et al*, 1996). Two mutations are needed within histone H4 to generate the *ts* phenotype: (1) lethal change at 82nd residue from T to I and (2) at 89th residue from A to V as an intragenic suppressor. The H4 82nd residue is located in the loop L2 that is bound to DNA. In consistent with the mutation site, transcription is affected in mutant cells. These mutant phenotypes are somewhat reminiscent to those of *htb1-72*, but quite different with regard to its strong genetic interactions with centromere-related gene *CSE4* (similar to CENP-A). Apparently, the budding yeast H4 mutant displayed both phenotypes of *htb1-72* and *htb1-223*. In the budding yeast H2A substitution mutant (the residues 20th from S to F, and at 30th from G to D), the phenotypes similar to H4 were found, resulting in G2–M arrest and an increased rate of chromosome loss (Pinto and Winston, 2000). The centromere-specific chromatin structure is disrupted in the H2A and H4 histone mutants (Meluh *et al*, 1998; Pinto and Winston, 2000). Taken together, the present and the previous results of budding yeast and fission yeast histone mutant analyses indicate that histones H2A, H2B (and uH2B) and H4 in addition to CENP-A, a centromere-specific histone H3, play important roles in centromere/kinetochore functions.

Materials and methods

Strains, media, PCR primers and antibodies

S. pombe histone H2B mutant strains used were described previously (Yuasa *et al*, 2004). The complete YPD, the minimal EMM2 and the sporulation medium SPA were used (Moreno *et al*, 1991). The cell number was measured by the Sysmex F-800 (Toa Med. Elec. Co.). For isolation of mutant *htb1* gene and construction of plasmids pH2B and pRHP6, fragments of *htb1* gene and *rhp6* gene were amplified by the PCR method with the nucleotides 5′-CGCGGATCCAACGATGAAGCAGCGAATGG-3′ and 5′-CGCGGATCCAAACCACATCAACTTCGCAC-3′ (for *htb1*) and 5′-TCAATCACGTAGCAGCGC-3′ and 5′-TTGGGAACAGCCGTTGAG-3′ (for *rhp6*). Polyclonal antibodies against *S. pombe* histone H2B were prepared by immunizing rabbits using the amino-terminal peptide (SAAEKKPASKAPAGKA) as antigen. Anti-HA (12CA5) monoclonal antibodies (Boehringer) and antibodies against methylated histone H3 (Abcam; ab7766) and acetylated histones H3 and H4 (Upstate Inc., #06-598 and #06-599) were used.

Microscopy

Cells expressing the GFP-tagged genes integrated on the chromosome were fixed with methanol. For the missegregation assay, LacI-GFP-NLS bound near the *cen1* locus was expressed in the presence of thiamine (Nabeshima *et al*, 1997). The procedures for immunofluorescence microscopy were described by Hagan and Hyams

(1988). Cells were fixed with paraformaldehyde and stained by TAT1 antibodies (Woods *et al*, 1989).

Immunoblotting

One volume of *S. pombe* cell culture (containing 1×10^8 cells) was mixed with 1/4 volume of ice-chilled 100% trichloroacetic acid (TCA). The resulting mixture was collected by centrifugation, and the pellets were washed with 10% TCA, followed by cell disruption with glass beads in 10% TCA. After centrifugation at 8000 r.p.m. for 10 min at 4°C, the washed precipitates were resuspended in the SDS sample buffer containing 1 mM phenylmethylsulfonyl fluoride (PMSF) and boiled at 70°C for 30 min. After centrifugation at 14 000 r.p.m. for 10 min, the supernatant was used for SDS–PAGE and immunoblot.

Chromatin immunoprecipitation

CHIP was carried out as described (Saitoh *et al*, 1997; Takahashi *et al*, 2000). Cells cultured at 37°C were fixed by formaldehyde. For immunoprecipitation, cell extracts were prepared using the extraction buffer (25 mM HEPES–KOH at pH 7.5, containing 200 mM NaCl, 10% glycerol, 0.2% NP-40, protease inhibitors, 1 mM PMSF and 1% Trasylol). Antibodies conjugated with protein A–Sepharose were used.

Micrococcal nuclease digestion

The procedures for micrococcal nuclease digestion were according to Takahashi *et al* (1992). Cells cultured at 37°C for 7 h were used for preparing extracts and treated with micrococcal nuclease (250 U/ml; Worthington Biochem). Plasmids pKT110, pKT108 and pYC148 were used as hybridization probes for making the micrococcal digestion patterns.

Supplementary data

Supplementary data are available at *The EMBO Journal* Online.

Acknowledgements

We are grateful to Dr Kozo Ajiro for discussion and technical instruction. This study was supported by the CREST research grant from the Japan Science and Technology Agency (JST) and the COE research grant from the Ministry of Education, Culture, Sports, Science and Technology of Japan (MEXT). TM, TH and TN were supported by the 21st Century COE grant of the Graduate School of Biostudies, from the MEXT. TN is a recipient of post-doctoral fellowships of the Japan Society for Promotion of Science (JSPS).

References

Cam HP, Sugiyama T, Chen ES, Chen X, FitzGerald PC, Grewal SI (2005) Comprehensive analysis of heterochromatin- and RNAi-mediated epigenetic control of the fission yeast genome. *Nat Genet* **37:** 809–819

Ekwall K, Cranston G, Allshire RC (1999) Fission yeast mutants that alleviate transcriptional silencing in centromeric flanking repeats and disrupt chromosome segregation. *Genetics* **153:** 1153–1169

Ekwall K, Javerzat JP, Lorentz A, Schmidt H, Cranston G, Allshire R (1995) The chromodomain protein Swi6: a key component at fission yeast centromeres. *Science* **269:** 1429–1431

Ekwall K, Nimmo ER, Javerzat JP, Borgstrom B, Egel R, Cranston G, Allshire R (1996) Mutations in the fission yeast silencing factors *clr4*$^+$ and *rik1*$^+$ disrupt the localisation of the chromo domain protein Swi6p and impair centromere function. *J Cell Sci* **109** (Part 11)**:** 2637–2648

Elgin SC, Workman JL (2002) Chromosome and expression mechanisms: a year dominated by histone modifications, transitory and remembered. *Curr Opin Genet Dev* **12:** 127–129

Feng Q, Wang H, Ng HH, Erdjument-Bromage H, Tempst P, Struhl K, Zhang Y (2002) Methylation of H3-lysine 79 is mediated by a new family of HMTases without a SET domain. *Curr Biol* **12:** 1052–1058

Fischle W, Wang Y, Allis CD (2003a) Binary switches and modification cassettes in histone biology and beyond. *Nature* **425:** 475–479

Fischle W, Wang Y, Allis CD (2003b) Histone and chromatin cross-talk. *Curr Opin Cell Biol* **15:** 172–183

Goshima G, Saitoh S, Yanagida M (1999) Proper metaphase spindle length is determined by centromere proteins Mis12 and Mis6 required for faithful chromosome segregation. *Genes Dev* **13:** 1664–1677

Grewal SI, Bonaduce MJ, Klar AJ (1998) Histone deacetylase homologs regulate epigenetic inheritance of transcriptional silencing and chromosome segregation in fission yeast. *Genetics* **150:** 563–576

Grewal SI, Elgin SC (2002) Heterochromatin: new possibilities for the inheritance of structure. *Curr Opin Genet Dev* **12:** 178–187

Hagan IM, Hyams JS (1988) The use of cell division cycle mutants to investigate the control of microtubule distribution in the fission yeast *Schizosaccharomyces pombe*. *J Cell Sci* **89:** 343–357

Hayashi T, Fujita Y, Iwasaki O, Adachi Y, Takahashi K, Yanagida M (2004) Mis16 and Mis18 are required for CENP-A loading and histone deacetylation at centromeres. *Cell* **118:** 715–729

Kitamura K, Katayama S, Dhut S, Sato M, Watanabe Y, Yamamoto M, Toda T (2001) Phosphorylation of Mei2 and Ste11 by Pat1 kinase inhibits sexual differentiation via ubiquitin proteolysis and 14-3-3 protein in fission yeast. *Dev Cell* **3:** 389–399

Korber P, Horz W (2004) SWRred not shaken; mixing the histones. *Cell* **117:** 5–7

Kornberg RD, Lorch Y (1999) Twenty-five years of the nucleosome, fundamental particle of the eukaryote chromosome. *Cell* **98:** 285–294

Luger K (2003) Structure and dynamic behavior of nucleosomes. *Curr Opin Genet Dev* **13:** 127–135

Luger K, Mader AW, Richmond RK, Sargent DF, Richmond TJ (1997) Crystal structure of the nucleosome core particle at 2.8 Å resolution. *Nature* **389:** 251–260

Matsumoto S, Yanagida M (1985) Histone gene organization of fission yeast: a common upstream sequence. *EMBO J* **4:** 3531–3538

Meluh PB, Yang P, Glowczewski L, Koshland D, Smith MM (1998) Cse4p is a component of the core centromere of *Saccharomyces cerevisiae*. *Cell* **94:** 607–613

Moreno S, Klar A, Nurse P (1991) Molecular genetic analysis of fission yeast *Schizosaccharomyces pombe*. *Methods Enzymol* **194:** 795–823

Nabeshima K, Nakagawa T, Straight AF, Murray A, Chikashige Y, Yamashita YM, Hiraoka Y, Yanagida M (1998) Dynamics of centromeres during metaphase-anaphase transition in fission yeast: Dis1 is implicated in force balance in metaphase bipolar spindle. *Mol Biol Cell* **9:** 3211–3225

Nabeshima K, Saitoh S, Yanagida M (1997) Use of green fluorescent protein for intracellular protein localization in living fission yeast cells. *Methods Enzymol* **283:** 459–471

Nakaseko Y, Nabeshima K, Kinoshita K, Yanagida M (1996) Dissection of fission yeast microtubule associating protein p93Dis1: regions implicated in regulated localization and microtubule interaction. *Genes Cells* **1:** 633–644

Ng HH, Feng Q, Wang H, Erdjument-Bromage H, Tempst P, Zhang Y, Struhl K (2002) Lysine methylation within the globular domain of histone H3 by Dot1 is important for telomeric silencing and Sir protein association. *Genes Dev* **16:** 1518–1527

Ohkura H, Kinoshita N, Miyatani S, Toda T, Yanagida M (1989) The fission yeast *dis2*$^+$ gene required for chromosome disjoining encodes one of two putative type 1 protein phosphatases. *Cell* **57:** 997–1007

Peterson CL, Laniel MA (2004) Histones and histone modifications. *Curr Biol* **14:** R546–R551

Pinto I, Winston F (2000) Histone H2A is required for normal centromere function in *Saccharomyces cerevisiae*. *EMBO J* **19:** 1598–1612

Polizzi C, Clarke L (1991) The chromatin structure of centromeres from fission yeast: differentiation of the central core that correlates with function. *J Cell Biol* **112:** 191–201

Richmond TJ, Davey CA (2003) The structure of DNA in the nucleosome core. *Nature* **423:** 145–150

Richmond TJ, Finch JT, Rushton B, Rhodes D, Klug A (1984) Structure of the nucleosome core particle at 7 Å resolution. *Nature* **311:** 532–537

Robzyk K, Recht J, Osley MA (2000) Rad6-dependent ubiquitination of histone H2B in yeast. *Science* **287:** 501–504

Saitoh S, Takahashi K, Yanagida M (1997) Mis6, a fission yeast inner centromere protein, acts during G1/S and forms specialized chromatin required for equal segregation. *Cell* **90:** 131–143

San-Segundo PA, Roeder GS (2000) Role for the silencing protein Dot1 in meiotic checkpoint control. *Mol Biol Cell* **11:** 3601–3615

Schalch T, Duda S, Sargent DF, Richmond TJ (2005) X-ray structure of a tetranucleosome and its implications for the chromatin fibre. *Nature* **436:** 138–141

Scott KC, Merrett SL, Willard HF (2006) A heterochromatin barrier partitions the fission yeast centromere into discrete chromatin domains. *Curr Biol* **16:** 119–129

Smith MM, Yang P, Santisteban MS, Boone PW, Goldstein AT, Megee PC (1996) A novel histone H4 mutant defective in nuclear division and mitotic chromosome transmission. *Mol Cell Biol* **16:** 1017–1026

Tagami H, Ray-Gallet D, Almouzni G, Nakatani Y (2004) Histone H3.1 and H3.3 complexes mediate nucleosome assembly pathways dependent or independent of DNA synthesis. *Cell* **116:** 51–61

Takahashi K, Chen ES, Yanagida M (2000) Requirement of Mis6 centromere connector for localizing a CENP-A-like protein in fission yeast. *Science* **288:** 2215–2219

Takahashi K, Murakami S, Chikashige Y, Funabiki H, Niwa O, Yanagida M (1992) A low copy number central sequence with strict symmetry and unusual chromatin structure in fission yeast centromere. *Mol Biol Cell* **3:** 819–835

Takahashi K, Murakami S, Chikashige Y, Niwa O, Yanagida M (1991) A large number of tRNA genes are symmetrically located in fission yeast centromeres. *J Mol Biol* **218:** 13–17

Takahashi K, Yamada H, Yanagida M (1994) Fission yeast minichromosome loss mutants mis cause lethal aneuploidy and replication abnormality. *Mol Biol Cell* **5:** 1145–1158

van Leeuwen F, Gafken PR, Gottschling DE (2002) Dot1p modulates silencing in yeast by methylation of the nucleosome core. *Cell* **109:** 745–756

van Holde KE (1988) *Chromatin*. New York: Springer-Verlag

Vijay-Kumar S, Bugg CE, Cook WJ (1987) Structure of ubiquitin refined at 1.8 Å resolution. *J Mol Biol* **194:** 531–544

Volpe T, Schramke V, Hamilton GL, White SA, Teng G, Martienssen RA, Allshire RC (2003) RNA interference is required for normal centromere function in fission yeast. *Chromosome Res* **11:** 137–146

White CL, Suto RK, Luger K (2001) Structure of the yeast nucleosome core particle reveals fundamental changes in internucleosome interactions. *EMBO J* **20:** 5207–5218

Woods A, Sherwin T, Sasse R, MacRae TH, Baines AJ, Gull K (1989) Definition of indivisiual components within the cytoskeleton of *Trypanosoma brucei* by a library of monoclonal antibodies. *J Cell Sci* **93:** 491–500

Yamashita YM, Nakaseko Y, Samejima I, Kumada K, Yamada H, Michaelson D, Yanagida M (1996) 20S cyclosome complex formation and proteolytic activity inhibited by the cAMP/PKA pathway. *Nature* **384:** 276–279

Yuasa T, Hayashi T, Ikai N, Katayama T, Aoki K, Obara T, Toyoda Y, Maruyama T, Kitagawa D, Takahashi K, Nagao K, Nakaseko Y, Yanagida M (2004) An interactive gene network for securin-separase, condensin, cohesin, Dis1/Mtc1 and histones constructed by mass transformation. *Genes Cells* **9:** 1069–1082